Journal of Engineering Science and Technology
Vol. 7, No. 2 (2012) 257 - 279

A DIMENSIONLESS SOLUTION TO RADIATION AND TURBULENT NATURAL CONVECTION IN SQUARE AND RECTANGULAR ENCLOSURES

A. K. A. SHATI*, S. G. BLAKEY, S. B. M. BECK

Department of Mechanical Engineering, University of Sheffield,
Mappin Street, S1 3JD, UK
*Corresponding Author: abdulmaged.shati@yahoo.co.uk

Abstract

The effects of natural convection with and without the interaction of surface radiation in square and rectangular enclosures have been studied, numerically and theoretically. The analyses were carried out over a wide range of enclosure aspect ratios ranging from 0.0625 to 16, including square enclosures in sizes from 40cm to 240cm, with cold wall temperatures ranging from 283 to 373 K, and hot to cold temperature ratios ranging from 1.02 to 2.61. The work was carried out using four different fluids whose properties are varying with temperature. FLUENT software was used to carry out the numerical study. Turbulence was modelled using the RNG k-ε model with a non-uniform grid. The Discrete Transfer Radiation Model (DTRM) was used for radiation simulation. A correlation equation for the new dimensionless group represented by the ratio of natural convection to radiation, as a function of Nusselt, Grashof, Prandtl numbers and temperature ratio also, the average Nusselt number without radiation as a function of Grashof and Prandtl numbers have been provided along with the constants needed to use them as a function of temperature ratio. This provides a generalised equation for heat transfer in square and rectangular enclosures both with and without radiation.

Keywords: Radiation interaction, Natural convection, Square and rectangular enclosures, Heat transfer, Aspect ratio.

1. Introduction

Heat transfer by natural convection inside enclosed spaces with radiation interaction is of practical interest in many engineering applications, such as the design of buildings for thermal comfort, nuclear reactors, solar collectors, and the

Nomenclatures

Br	Brinkman number, $= \mu U^2 / k\Delta T$
C_p	Specific heat capacity, J/kgK
Gr	Grashof number, $= \beta g \Delta T L^3 \rho^2 / \mu^2$
g	Gravitational acceleration, m/s^2
H	Heat transfer rate, W
h	Heat transfer coefficient, W/m^{2}K
I	Radiation heat transfer intensity, W/m^2
K	Thermal conductivity of the fluid, W/mK
L	Enclosure wall length, m
Nu_c	Convection Nusselt number, $= Q_{conv} / Q_{cond} = hH / k$
Nu_r	Radiation equivalent Nusselt number, $= Q_{rad} / Q_{cond}$
Nu_t	Total Nusselt number, $= (Q_{conv} + Q_{rad}) / Q_{cond}$
Pr	Prandtl number, $= \mu C_p / k$
Q_{cond}	Conduction heat transfer, W
Q_{conv}	Convection heat transfer, W
Q_{rad}	Radiation heat transfer, W
Ra	Rayleigh number, $= g\beta\Delta T L^3 / \nu\alpha$
RC_n	The new dimensionless group, $= Nu_c / Nu_r = Q_{conv} / Q_{rad} \approx h / \sigma f_{(L,\varepsilon)} T^3$
S_h	Any other heat sources, W/m^3
T	Temperature, K
T_r	Temperature ratio, $= T_h / T_c$
u_τ	Shear velocity ($= \sqrt{\tau_w / \rho}$), m/s
x, y	Horizontal and vertical coordinates, m
y^+	Dimensionless distance, $= \rho u_\tau y / \mu$

Greek Symbols

α	Thermal diffusivity, m^2/s
β	Thermal expansion coefficient, 1/K
ΔT	Temperature difference between hot and cold walls, K
ν	Kinematic viscosity, m^2/s
ε	Surface emissivity
μ	Dynamic viscosity, Ns/m^2
σ	Stefan-Boltzman constant (=5.672×10^{-9}), W/m^{2}K^4
τ_w	Local wall shear stress, N/m^2
ρ	Density, kg/m^3
Ω	Hemispherical solid angle, rad

cooling of electronic equipment [1]. In a rectangular enclosure with natural convection as shown in Fig. 1, the internal flow is dominated by buoyancy forces. The most important dimensionless group in natural convection inside this enclosure is the Rayleigh number (which is the ratio of buoyancy forces and the viscous forces acting on a fluid,) and is analogous to the Reynolds number for buoyancy dominated flows. The value of the Rayleigh number can indicate whether the flow can be considered as laminar or turbulent [2]. Inside enclosures,

transition from laminar to turbulent flow occurs when the Rayleigh number is greater than one million [3].

The interest in this problem over the last four decades has led to many numerical and experimental studies. De Vahl Davis [4] provided a bench-mark numerical solution for the natural convection of air in a square cavity and compared this to 37 other pieces of work. Barletta et al. [5] numerically studied the laminar natural convection in a 2-D enclosure. A good agreement between the solutions was found by comparison to the bench-mark results. Ramesh and Venkateshan [6] investigated experimentally the natural convection in a square enclosure using a differential interferometer and again provided a correlation equation to calculate the average convection Nusselt number. Lankhorst et al. [7] experimentally studied the buoyancy induced flows in a differentially heated air filled square enclosure at high Rayleigh numbers. They found that the core stratification has a significant influence on the regimes and the characteristics of the flow. Nor Azwadi and Tanahashi [8] proposed a three-dimensional thermal lattice Boltzmann model to simulate incompressible thermal flow. Their results on laminar natural convection in a cubic cavity agreed well with previous studies.

Many papers have been published that discuss the turbulent natural convection in the absence of radiation in enclosures. Henekes et al. [9] studied numerically the laminar and turbulent natural convection flow in a two dimensional square cavity using three different turbulence models. They have shown that the k-ε model gives too high a prediction, whereas the low Reynolds number models are reasonably close to the experiment. Markatos and Perlicleous [3] have reported on laminar and turbulent buoyancy driven flows and heat transfer in an enclosed cavity. Henkes and Hoogendoorn [10] published a numerical reference solution for turbulent natural convection in a differentially heated enclosure at $Ra=5\times10^{10}$, by a comparison of the computational results of 10 different groups.

The importance of surface radiation with natural convection in enclosures has also been studied and investigated by many researchers. Balaji and Venkateshan [11] numerically investigated the interaction of surface radiation with laminar free convection in a square cavity. They elucidate the importance of surface radiation even at low emissivities and provide some reasons for the discrepancies noticed between the experimental and theoretical correlations. Sen and Sarkar [12] have considered the effects of variable fluid properties on the interaction of laminar natural convection and surface radiation in a differentially heated square cavity. They discovered that the presence of both radiation at low emissivity ($\varepsilon = 0.1$) and variable properties, intensively affect the thermal stratification of the core and the symmetry of the mid-plane vertical velocity as well as temperature profiles.

Velusamy et al. [13] studied the turbulent natural convection with the effect of surface radiation in square and rectangular enclosures. They pointed out that the radiation heat transfer is significant even at low temperatures and low emissivities. Colomer et al. [14] looked at the three-dimensional numerical simulation of the interaction between the laminar natural convection and the radiation in a differentially heated cavity for both transparent and participating media. Their work reveals that in a transparent fluid, the radiation significantly increases the heat flux across the enclosure. Kumar and Eswaran [15] numerically studied the combined radiation and laminar natural convection in a differential heated cubic cavity. They found that the wall emissivity has a strong influence on

the heat transfer. Sharma et al. [1] investigated and analysed turbulent natural convection with thermal surface radiation in inclined square enclosures. They reported that, for the case of an angle of inclination $\varphi = 90°$, the circulation rate in the enclosure increases significantly and the turbulent viscosity is three times that of the non-radiating case.

Elsherbiny et al. [16] reported experimentally the laminar natural convection across vertical and inclined air layers for different enclosure aspect ratios. They provided correlation equations to calculate Nusselt numbers. Shati et al. [17] experimentally studied the effect of aspect ratio on the heat transfer between two parallel plates. They found that the heat transfer was increased gradually by decreasing the aspect ratio. Patterson and Imberger [18] studied the transient natural convection in a cavity of aspect ratios less than one. They provide a scaling analysis of the heat transfer inside a rectangular enclosure. Bejan [19] explained the pure natural convection heat transfer flow regimes in tall, square and shallow enclosures. He claims that the relationship between Nusselt number and Rayleigh number in enclosures with different aspect ratios is more complicated and cannot be expressed by just a power law.

From the existing literature, it is apparent that the problem of laminar and turbulent natural convection with realistic conditions; such as variable properties with radiation interaction and also with changing the temperatures of the cold and hot walls require more investigations. The present work which studies the effect of realistic conditions (which include the effect of different enclosure size, aspect ratio, changing the cold and hot wall temperatures, and using different fluids, for all properties vary with temperature) on the turbulent natural convection with and without surface radiation reports a correlation equation for the natural convection for both types of case. The analysis uses a new dimensionless group which demonstrates the relation between the convection and radiation heat transfer inside the square and rectangular enclosures.

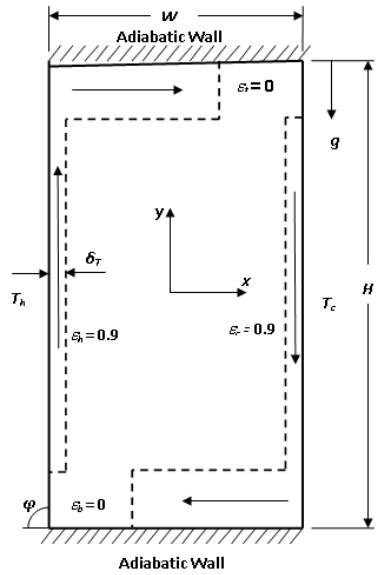

Fig. 1. Schematic Diagram of the Rectangular Enclosure.

2. Mathematical Model

The system that was solved is shown schematically in Fig. 1. This is a two dimensional flow of an ideal gas in a rectangular enclosure of height H and length W. The two vertical hot and cold walls are heated isothermally and the other two (horizontal) walls are adiabatic. To simplify the problem and focus on the heat transfer between the hot and cold walls the adiabatic wall surfaces are taken as zero emissivity which is similar to a highly shiny, insulated surface. The turbulent flow in the enclosure is analysed using the commercial code (FLUENT 6.3) and by using the RNG k-ε model with the Boussinesq approximation for the density.

Zhang et al. [20] have compared four turbulence models for the turbulent natural convection in enclosures they found that the RNG k-ε model agreed better with the experimental results of [24] than the other models. Zhang et al. [21] compared eight turbulence models for predicting airflow and turbulence in enclosed environments they have found that when comparing the RANS models, the RNG k-ε model produced the best results. For these reasons the RNG k-ε model was chosen in this work, where equations used by the model (from [22]), incorporate free convection in the Cartesian coordinate, these are given below:

Continuity equation

$$\frac{\partial(\rho)}{\partial t}+\frac{\partial(\rho u)}{\partial x}+\frac{\partial(\rho v)}{\partial y}=0 \tag{1}$$

Momentum equations

$$\frac{\partial(\rho u)}{\partial t}+\frac{\partial(\rho uu)}{\partial x}+\frac{\partial(\rho uv)}{\partial y}=-\frac{\partial p}{\partial x}+\frac{\partial}{\partial y}\left[\mu_{eff}\left(\frac{\partial u}{\partial y}+\frac{\partial v}{\partial x}\right)\right] \tag{2}$$

$$\frac{\partial(\rho v)}{\partial t}+\frac{\partial(\rho uv)}{\partial x}+\frac{\partial(\rho vv)}{\partial y}=-\frac{\partial p}{\partial y}+\frac{\partial}{\partial x}\left[\mu_{eff}\left(\frac{\partial v}{\partial x}+\frac{\partial u}{\partial y}\right)\right]+\rho\beta g(T-T_o) \tag{3}$$

where $\rho\beta g(T-T_o)$ is the Boussinesq approximation for buoyancy, and the energy equation

$$\frac{\partial(\rho CpT)}{\partial t}+\frac{\partial(\rho uCpT)}{\partial x}+\frac{\partial(\rho vCpT)}{\partial y}=\frac{\partial}{\partial x}\left[K_{eff}\frac{\partial T}{\partial x}\right]+\frac{\partial}{\partial y}\left[K_{eff}\frac{\partial T}{\partial y}\right]+S_h \tag{4}$$

The turbulent kinetic energy equation is also incorporated with these

$$\frac{\partial(\rho ku)}{\partial x}+\frac{\partial(\rho kv)}{\partial y}=\frac{\partial}{\partial x}\left[\left(\propto_k \mu_{eff}\right)\frac{\partial k}{\partial x}\right]+\frac{\partial}{\partial y}\left[\left(\propto_k \mu_{eff}\right)\frac{\partial k}{\partial y}\right]+G_k+G_b-\rho\epsilon \tag{5}$$

and the dissipation rate equation

$$\frac{\partial(\rho\epsilon u)}{\partial x}+\frac{\partial(\rho\epsilon v)}{\partial y}=\frac{\partial}{\partial x}\left[\left(\propto_\epsilon \mu_{eff}\right)\frac{\partial k}{\partial x}\right]+\frac{\partial}{\partial y}\left[\left(\propto_\epsilon \mu_{eff}\right)\frac{\partial k}{\partial y}\right]+C_{1\epsilon}\frac{\epsilon}{k}(G_k+C_{3\epsilon}G_b)-C_{2\epsilon}^{*}\rho\frac{\epsilon^2}{k} \tag{6}$$

In the near wall region, the solution variables changes greatly with large gradients. Therefore, to successfully determine and predict the turbulent flow, precise representations of the flow in the near wall region were needed [22].

So, to represent and capture the critical importance of the buoyancy flow features in the simulation model, the two-layer model was employed for the near-wall treatment with the RNG k-ε model where the viscous-affected near-wall region (at $Re_y < 200$) was solved using the one equation model of Wolfsten [22].

The Discrete Transfer Radiation Model (DTRM), which was used in the present study, is a relatively simple model which, used for calculating radiation which can be used both with and without opacity in the fluid. It applies to a wide range of optical thicknesses, and its accuracy can be increased by increasing the number of rays [22].

Turbulence has a strong interaction with the mean flow features, so, the turbulent flow results tend to be grid dependant. Thus, a sufficiently fine grid is needed in the regions where the mean flow features has severe changes. For the models used in this study, different non-uniform mesh sizes were used to get acceptable results. The grid size was from 67×67 up to 200×200 for the square enclosure. For rectangular enclosure the grid size was from 100×19 for the aspect ratio 16 up to 100×400 for the aspect ratios 0.0625. The height of the enclosure was kept the same for all aspect ratios.

The segregated solver was used with the two layer model for calculating the boundary and a sufficient fine grid near the walls and a relatively coarse grid at the core. The SIMPLE algorithm for a pressure velocity coupling was used with a second order upwind discretization method for solving the momentum and energy equations.

The grid independency has been studied for the case of temperature ratio $T_r = 2.6$ and an enclosure size of 240cm square using Hydrogen as a working fluid. The analysis was done for three non-uniform grid patterns 80×80, 100×100 and 150×150 nodes, taking the total average Nusselt number as the parameter to be compared. The results varied by less than 3% for this square enclosure. For rectangular enclosures, the grid independence has been studied for the case of temperature ratio $T_r = 2.6$ and an enclosure size of 60x3.75cm using air as a working fluid. The analysis was done for three non-uniform grid patterns 100×19, 150×29 and 200×39 nodes, taking the total average Nusselt number as the parameter to be compared. The results were found to vary by less than 1.2%.

3. Dimensional Analysis

This study focuses on the dimensional analysis for two cases of natural convection, pure natural convection and natural convection with interaction of surface thermal radiation. Both problems have been analysed and correlation equations are provided for both cases below.

From Fig. 1 the governing equations for the mass, momentum and energy conservation within the enclosure can be described as in Eqs. (1) to (4) in the mathematical model above.

By multiplying Eq. (2) by $\frac{\partial}{\partial y}$ and Eq. (3) by $\frac{\partial}{\partial x}$ then the pressure terms can be eliminated and the momentum equations combined to produce a single momentum equation:

$$\frac{\partial}{\partial x}\left(\frac{\partial v}{\partial t}+u\frac{\partial v}{\partial x}+v\frac{\partial v}{\partial y}\right)-\frac{\partial}{\partial y}\left(\frac{\partial u}{\partial t}+u\frac{\partial u}{\partial x}+v\frac{\partial u}{\partial y}\right) = \vartheta\left[\frac{\partial}{\partial x}\left(\frac{\partial^2 v}{\partial x^2}+\frac{\partial^2 v}{\partial y^2}\right)-\frac{\partial}{\partial y}\left(\frac{\partial^2 u}{\partial x^2}+\frac{\partial^2 u}{\partial y^2}\right)\right]+g\beta\frac{\partial T}{\partial x} \quad (7)$$

Which contains three momentum groups that control the flow of air in the enclosure; these groups are, from left: inertia, viscous friction, and buoyancy. Based on Fourier's law, the radiation heat transfer at the boundary can be defined as:

$$-k\frac{\partial T}{\partial x}\Big|_{wall1}=-k\frac{\partial T}{\partial x}\Big|_{wall2}=h(T_{wall1}-T_{wall2})+f_{(L,\varepsilon)}\sigma(T_{wall1}^4-T_{wall2}^4) \quad (8)$$

where $f_{(L,\varepsilon)}$ is a function of the geometry and separation of the walls and their emissivities, ε is the Stephan-Boltzmann constant.

The above equations of motion can be simplified with a dimensional analysis. Patterson and Imberge [18] proposed that the energy equation can be converted to dimensionless groups at a time just after $t=0$ when the fluid beside each wall is motionless ($u=v=0$) and the thermal boundary layer thickness, δ_T is much smaller than the enclosure height so that:

$$\frac{\partial^2 T}{\partial y^2}\ll\frac{\partial^2 T}{\partial x^2}$$

Therefore the energy equation (4) can be simplified to:

$$\frac{\partial T}{\partial t}=\alpha\left(\frac{\partial^2 T}{\partial x^2}\right) \quad (9)$$

or $$\frac{\Delta T}{t}\propto\alpha\frac{\Delta T}{{\delta_T}^2}$$

This equation indicates that following $t=0$, the thermal boundary layer increases proportionally to:

$$\delta_T\sim(\alpha t)^{1/2} \quad (10)$$

Referring to Eq. (7), Bejan [19] argues that by assuming $u\ll v$ the initial vertical velocity scale will be as:

$$v=\frac{g\beta\Delta T\alpha t}{\vartheta} \quad (11)$$

As time passes, a steady state situation occurs, where the flow is dominated by buoyancy effects. There will be a time, $t=t_f$ when the boundary layer reaches its maximum thickness and an energy balance occurs between heat conducted from the wall and the heat carried away by the buoyancy. From the energy equation (4) it is possible to define this time as:

$$t_f=\left(\frac{\vartheta H}{g\beta\Delta T\alpha}\right)^{-1/2} \quad (12)$$

The governing equations can be non-dimensionalised using the following scale groups as recommended by Bejan [19] with some change in θ, where the hot and cold wall temperatures are used:

$$X = \frac{x}{\delta_T}, Y = \frac{y}{H}, \qquad \theta = \frac{(H/W)T_h(T - T_c)}{T_c(T_h - T_c)}, \qquad U = \frac{u}{(\delta_T/H)v_f} \; and \; V = \frac{v}{v_f}$$

The resulting non-dimensionless governing equations are as Bejan [19]:

$$\frac{\partial U}{\partial X} + \frac{\partial V}{\partial Y} = 0 \tag{13}$$

$$\frac{1}{Pr}\left[\frac{\partial}{\partial X}\left(U\frac{\partial V}{\partial X} + V\frac{\partial V}{\partial Y}\right) - Gr^{-\frac{1}{2}}Pr^{-\frac{1}{2}}\frac{\partial}{\partial Y}\left(U\frac{\partial U}{\partial X} + V\frac{\partial U}{\partial Y}\right)\right]$$
$$= \frac{\partial}{\partial X}\left(\frac{\partial^2 V}{\partial X^2} + Gr^{-\frac{1}{2}}Pr^{-\frac{1}{2}}\frac{\partial^2 V}{\partial Y^2}\right) - Gr^{-\frac{1}{2}}Pr^{-\frac{1}{2}}\frac{\partial}{\partial X}\left(\frac{\partial^2 U}{\partial X^2} + Gr^{-\frac{1}{2}}Pr^{-\frac{1}{2}}\frac{\partial^2 U}{\partial Y^2}\right)$$
$$+ AR^{-1}T_r{}^{-1}\frac{\partial \theta}{\partial X} \tag{14}$$

$$U\frac{\partial \theta}{\partial X} + V\frac{\partial \theta}{\partial Y} = \frac{\partial^2 \theta}{\partial X^2} + Gr^{-\frac{1}{2}}Pr^{-\frac{1}{2}}\frac{\partial^2 \theta}{\partial Y^2} \tag{15}$$

and from the heat transfer at the boundary shown in Eq. (8):

$$-\frac{\partial \theta}{\partial X}\Big|_{wall} = \left(\frac{\delta_T}{H}\right)\left(\frac{T_h}{T_c}\right)[Nu_c + Nu_r] \tag{16}$$

where Nu_c is the modified convection Nusselt number:

$$Nu_c = \frac{hL}{k} * AR \tag{17}$$

and Nu_r is the modified Radiation equivalent Nusselt number:

$$Nu_r = \frac{f_{(L,\varepsilon)}\sigma H(T_h^4 - T_c^4)}{k(T_h - T_c)} * AR \tag{18}$$

where AR is the aspect ratio

$$AR = \frac{H}{W} \tag{19}$$

and the total Nusselt number is

$$Nu_t = Nu_c + Nu_r \tag{20}$$

also the absolute temperature ratio T_r is defined as

$$T_r = \frac{T_h}{T_c} \tag{21}$$

The two numbers from Eqs. (17) and (18) could be combined into a new dimensionless group RC_n, which is the ratio of convection heat transfer to surface radiation:

$$RC_n = \frac{Nu_c}{Nu_r} = \frac{h(T_h - T_c)}{f_{(L,\varepsilon)}\sigma(T_h^4 - T_c^4)} \approx \frac{h}{\sigma f_{(L,\varepsilon)}T^3} \tag{22}$$

Thus dimensionless groups defined above can be combined into the following generalised dimensionless equation:

$$Nu_t = \varphi(RC_n, Gr, Pr, T_r, AR) \tag{23}$$

or

$$RC_n = \varphi(Nu_t, Gr, Pr, T_r, AR) \tag{24}$$

where RC_n is the heat transfer ratio in terms of total Nusselt number, Grashof number, Prandtl number, absolute temperature ratio and aspect ratio.

Equation (23) can be compared to Johnstone and Thring's [23] dimensionless equation for a general heat transfer problem involving radiation, convection and conduction using the Thring number $\left(Th = \frac{\rho c_p v}{\sigma \varepsilon T^3}\right)$:

$$Nu = \varphi(Re, Gr, Pr, Th, T_r) \tag{25}$$

For the case of natural convection without radiation interaction; by setting $\mathrm{Nu_r}$ to zero from Eq. (16) and hence omitting RC_n from Eq. (23) it gives:

$$Nu_c = \emptyset(Gr, Pr, T_r, AR) \tag{26}$$

From this, the following correlation equation for natural convection without radiation interaction in a square enclosure is formed by putting $AR = 1.0$. This forms a relationship between the average Nusselt, Grashof and Prandtl numbers in the square enclosure:

$$Nu_c = \frac{k_1 Gr^{a_1}}{Pr^{b_1}} \tag{27}$$

where k_1, a_1 and b_1 are constants and are a function of the temperature ratio of the hot and cold walls of the enclosure.

Also, from Eq. (24) the following correlation equation for the natural convection with the interaction of thermal surface radiation has been provided which matches the relation between the new dimensionless group (natural convection to radiation heat transfer) and the total Nusselt number, Grashof number and Prandtl number in the square enclosure by putting $\mathrm{AR} = 1.0$

$$RCn = \frac{Q_{conv}}{Q_{rad}} = \frac{k_2 Gr^{b_2}}{{Nu_t}^{a_2} Pr^{c_2}} \tag{28}$$

where k_2, a_2, b_2 and c_2 are constants and are a function of the temperature ratio $\mathrm{T_r}$ of the hot and cold walls of the enclosure.

For the case of natural convection with radiation interaction in rectangular enclosure, the velocity contours, stream lines and isothermal lines for the aspect ratios 16, 8, 4, 2, 1.5, 1.0, 0.75 and 0.5 are shown in Fig. 2. These have been scaled horizontally so that they are all the same width. It can be seen that there are two flow regimes and a transition regime between them:

(i) From an aspect ratio greater than 1.5 up to 16 (and probably beyond),

(ii) The second one (transitional) regime is between aspect ratios of 1.5 and 0.75 and

(iii) The third regime is from an aspect ratio less than 0.75 down to 0.0625 (and again probably beyond).

According to the numerical results of the rectangular enclosure with different aspect ratios in this study, the transition regime can be included into other two regimes:

(i) Regime one starts from square to tall enclosures for aspect ratio ranging from 1 to 16,

(ii) Regime two starts from square to shallow enclosures for aspect ratio ranging from 1 to 0.0625.

From Eq. (26) above, the following correlation equation for natural convection without radiation interaction in rectangular enclosure is formed. This forms a relationship between the average Nusselt, Grashof, Prandtl numbers and aspect ratio in rectangular enclosures:

$$Nu_c = \frac{k_1 Gr^{a_1}}{Pr^{b_1}} * f(AR) \tag{29}$$

where k_1, a_1 and b_1 are as given in Eq. 27, and $f(AR)$ is the aspect ratio conversion equation and it has two forms for each regime:

For the first regime (aspect ratio from 1 to 16)

$$f(AR) = AR^{ka1} + ka2e^{AR^{ka3}} + ka4 \tag{30}$$

For the second regime (aspect ratio from 1 to 0.0625)

$$f(AR) = kb1\left(AR^{kb2} + kb3e^{AR^{kb4}} + kb5\right) \tag{31}$$

where ka_1, ka_2, ka_3 and ka_4 and kb_1, kb_2, kb_3, kb_4 and kb_5 are constants and are a function of the temperature ratio T_r of the hot and cold walls of the rectangular enclosure.

Also, from Eq. (24) above, the following correlation equation for the case of natural convection with the interaction of thermal surface radiation in rectangular enclosure has been provided which matches the relationship between the new dimensionless group and the total Nusselt number, Grashof number, Prandtl number and the aspect ratio in the rectangular enclosure

$$RCn = \frac{Q_{conv}}{Q_{rad}} = \frac{k_2 Gr^{b_2}}{{Nu_t}^{a_2} Pr^{c_2}} * f(AR) \tag{32}$$

where k_2, a_2, b_2 and c_2 are as given in Eq. 28. Here $f(AR)$ is also the aspect ratio conversion equation and it has two forms for each regime:

For the first regime (aspect ratio from 1 to 16)

$$f(AR) = AR^{kc1} + kc2e^{AR^{kc3}} + kc4 \tag{33}$$

For the second regime (aspect ratio from 1 to 0.0625)

$$f(AR) = kd1\left(AR^{kd2} + kd3e^{AR^{kd4}} + kd5\right) \tag{34}$$

where kc_1, kc_2, kc_3 and kc_4 and kd_1, kd_2, kd_3, kd_4 and kd_5 are constants and are a function of the temperature ratio T_r of the hot and cold walls of the rectangular enclosure.

4. Results and Discussion

To validate the computational model described in the mathematical model section, the average Nusselt number results of a numerical solution have been compared with the predicted results of Markatos and Pricleous [3]. The results are also compared with the correlation equation obtained from the experimental results by Elsherbiny et al. [16]. These are all displayed in Table 1, where it can be seen that the present results are more consistent with the experimental correlations than other numerical results.

Table 1. Average Nusselt Number as a Comparison with Others for Natural Convection in a Square Enclosure.

Ra	Present results (Numerical)	Elsherbiny et al. [16] (Experimental)	Markatos and Pericleous [3] (Numerical)
10^8	31.42	28.78	38.06
10^9	66.16	62	74.96
10^{10}	135.15	133.57	159.89

For further validation of the model used, the problem of natural convection without radiation interaction in a square enclosure was solved for a high Rayleigh Number ($5x10^{10}$). The results were compared with the experimental results provided by both Cheesewright et al. [24] and King [25] and also with a reference solution from 10 research groups provided by Heneks and Hoogendoorn [10] as shown in Table 2. The results were compared for the average Nusselt number and for the local Nusselt number at the mid height of the enclosure. It can be seen from Table 2 that the present results are agreed well with the average value of the experimental results from the reference solution [10].

Table 2. Average and Mid-height Nusselt Number for Natural Convection in a Square Enclosure at $Ra=5\times10^{10}$ as a Comparison with Reference and Experimental Results.

Quantity	Present results (Numerical)	Henkes and Hoogendoorn [10] (Numerical)	Cheesewright et al. [24] and King [25] (Experimental)
Average Nu	194.9	256	154-210(average=182)
Mid height Nu	205	261	133-241(average=187)

In order to make the preceding analysis more useful and general, a large number of simulations were performed to extract the numerical relationship between the dimensionless numbers. To this end, the interaction effects of turbulent natural convection with and without surface thermal radiation on fluid flow in square and rectangular enclosures are studied in detail.

The results are divided into three groups for square enclosure and two flow regimes for rectangular enclosure according to the aspect ratio:

For square enclosures:

- different cold wall temperatures (ranging from 283 to 373 K) to cover a wide range of temperatures and this could be extended if needed,
- different enclosure sizes (ranging from 40 cm square to 240 cm square) and
- different fluid properties.

For rectangular enclosures the regimes are as described above.

For all of the three groups for square enclosure and for the two regimes of rectangular enclosure the ratio between the hot and cold wall temperatures was in the range of ($T_r = \frac{T_h}{T_c} = 1.02\ to\ 2.61$) and the modelling was conducted with all the fluid properties as a function of temperature.

For the case of natural convection with radiation interaction in rectangular enclosure, shown in Fig. 2 the velocity contours, stream lines and isothermal lines for the aspect ratios 16, 8, 4, 2, 1.5, 1.0, 0.75 and 0.5. These have been scaled horizontally so that they are all the same width. It can be seen that there are the three flow regimes which are described above.

For the first regime it can be seen from Fig. 2(a) that the unsteady eddies observed at the top of the hot wall and at the bottom of the cold wall increase in size as the aspect ratio increases and the flow on the two vertical walls tends to exert more force on the stratified core. The core shrinks as the aspect ratio increases and the stream lines, as well as the isothermal lines, vary from the horizontal until they disappear. By now, the two boundary layers of the hot and cold walls merge together and the conduction heat transfer become dominant.

In the second flow regime the two hot and cold walls have balance effects on the core and show stratified transient flow in the core; this can be seen clearly from the stratified stream lines and isothermal lines as in Figs. 2(b) and (c). The core in the third flow regime can be seen in Fig. 2 to be unaffected from the two hot and cold walls flow boundary layers and the convection heat transfer becomes dominant as the radiation dramatically decreases with the decrease of aspect ratio.

The convection heat transfer decreases as the aspect ratio increases or decreases from the unity, Bejan [19] mentioned the same for laminar pure natural convection. This means that convection heat transfer decreases for both tall and shallow enclosures compared to the square enclosure. At the same time (for a fixed cavity height), radiation heat transfer is directly proportional to the aspect ratio, which means that radiation heat transfer increases with increasing aspect ratio.

Figures 3 and 4 show the relation between (*Qconv/Qrad*) and (T_r) for the three different groups of square enclosure and the two regimes of the rectangular enclosure. It can be seen from these figures that; as the T_r increases the (*Qconv/Qrad*) increases at the same time up to a value of T_r which is 1.2. Then for $T_r > 1.2$, (*Qconv/Qrad*) decreases as T_r continues to increases. This means that as the T_r increases, convection increases more than radiation heat transfer up to a T_r of 1.2 for all groups. At temperature ratios greater than 1.2, the radiation heat transfer becomes dominant, i.e. the radiation increases more than the convection and the ratio (*Qconv/Qrad*) decreases.

This is also because increasing the temperature will increase the viscosity of the fluid which will slow down the velocity in the hot wall region, which results in a reduction of the convection heat transfer. At the same time, increasing the

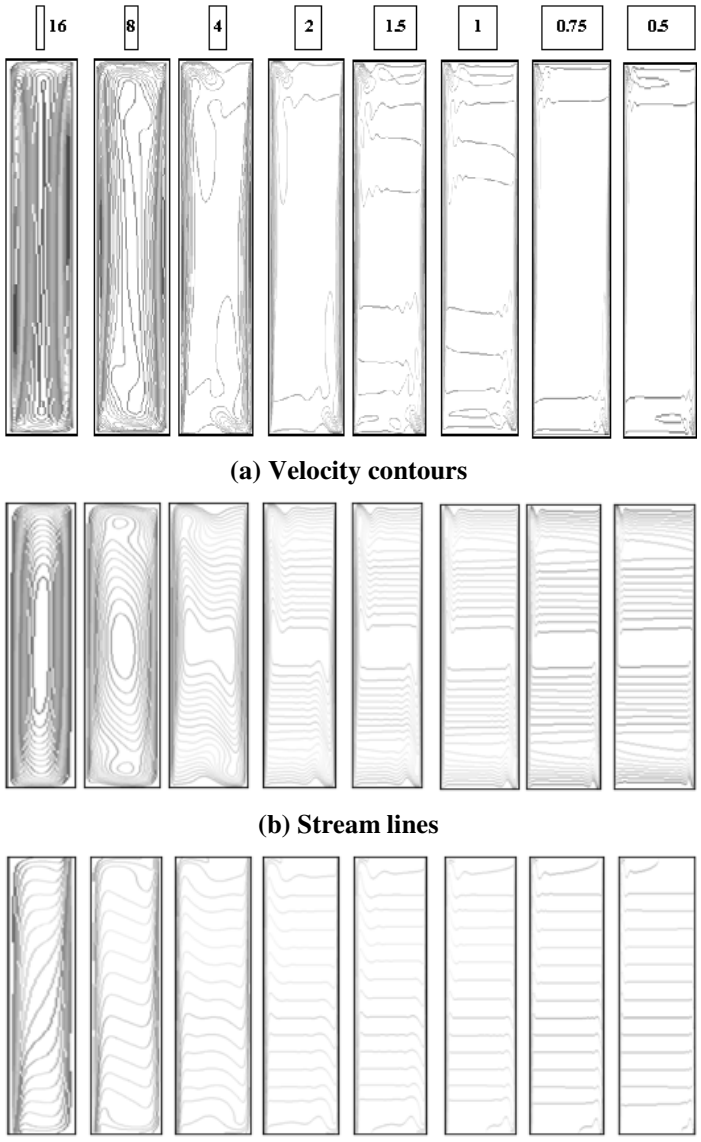

(a) Velocity contours

(b) Stream lines

(c) Isothermal lines

Fig. 2. Flow Profiles for Aspect Ratios 16, 8, 4, 2, 1.5, 1.0, 0.75 and 0.5: a) Velocity Contours, b) Stream Lines and c) Isothermal Lines.

temperature will increase the thermal conductivity which results in an increase of the convection heat transfer. It can be seen from Figs. 3(a) and (b) increasing the temperature and the size will increase the radiation more than the convection heat transfer, this results in a decrease of the overall of (*Qconv/Qrad*) as a function of T_r. This is because the radiation heat transfer is a function of T^4. Furthermore as shown in Fig. 3(c), increasing the thermal conductivity from 0.017 for Argon to 0.18 for Hydrogen will increase the convection heat transfer results increasing the overall of (*Qconv/Qrad*) as a function of T_r. Also from Fig. 4(a) it can be seen

that as the aspect ratio increase the ratio (*Qconv/Qrad*) as a function of T_r has a slightly decrease, on the other hand from Fig. 4(b) as the aspect ratio decrease the ratio (*Qconv/Qrad*) as a function of T_r has a dramatically increase.

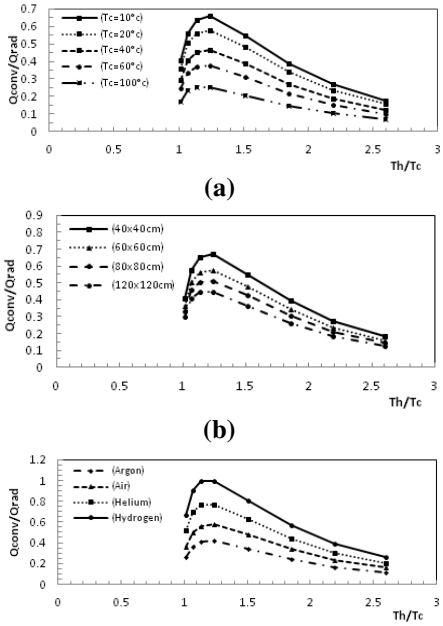

Fig. 3. Relation between *Qc/Qr* with respect to *Th/Tc* for Different (a) Cold Wall Temperatures, (b) Enclosure Sizes and (c) Fluids.

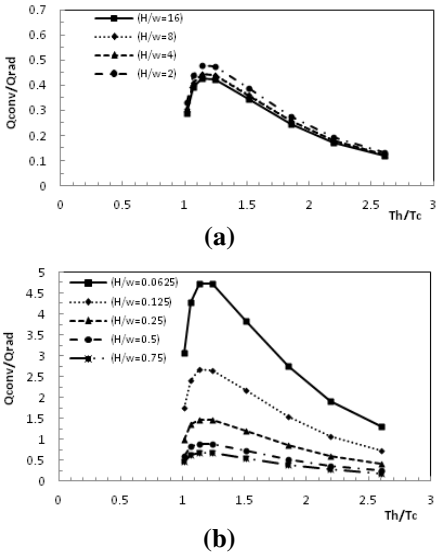

Fig. 4. Relation between Heat Transfer Ratio and Temperature ratio of: a) First Regime (Aspect Ratios from 1 to 16), and b) Second Regime (Aspect Ratios from 0.0625 to 1.)

The relation between the ratio of ($Ra^{1/3}/Nu$) and the temperature ratio T_r has the same trend as the relation between ($Qconv/Qrad$) and T_r, as shown in Fig. 5. This is because both of these two relations are increasing as a function of T and decreasing as a function of T^4. From Fig. 5 it can be seen that, as the temperature ratio increases, the ratio ($Ra^{1/3}/Nu$) increases until it reaches a value of T_r of 1.2; which is the same as before. After that, as T_r increases, the ratio of ($Ra^{1/3}/Nu$) decreases. This is because increasing the temperature will increase the dynamic viscosity and thermal conductivity linearly and decrease the density linearly; this causes the kinematic viscosity (υ) to increase quadratically, (i.e. function of T^2); because it is a function of dynamic viscosity and density, $(\upsilon = \mu/\rho)$. This results in a linear increase of the Nusselt number and a decrease of Rayleigh number as a function of $(1/\upsilon^2)$ (or a decrease of Rayleigh number as a function of T^4).

Also increasing the cold wall temperature will decrease the overall trend of ($Ra^{1/3}/Nu$) with T_r. This can be seen in Fig. 5(a). Also from Figs. 5(b) and (c), increasing the size of the enclosure and the gas properties (such as thermal conductivity and kinematic viscosity) results in an increase of the overall trend of ($Ra^{1/3}/Nu$) with respect to T_r.

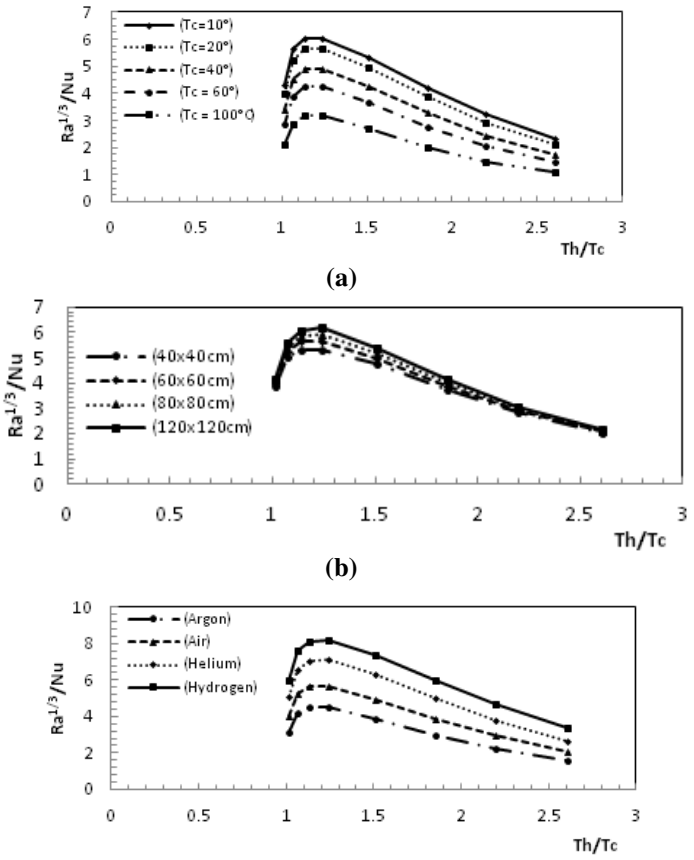

Fig. 5. Relation between $Ra^{1/3}/Nu$ with respect to T_h/T_c for Different (a) Cold Wall Temperatures, (b) Enclosure Sizes and (c) Fluids.

The identification of a new dimensionless group has arisen from the results of all three groups that were analysed. Each set of curves has collapsed into a single curve by using some exponents of the variables as conversion parameters. This can be seen by comparing Fig. 3 and Fig. 6. Here Figs. 3(a) and 6(a), the curves of the group collapsed into a single curve using only the cold wall temperature as a conversion factor. The same sort of results were obtained for the second and third groups by using different variables as conversion parameters, as shown in Figs. 3(b) and 6(b) and Fig. 3(c) and 6(c). From the similarity of the relationships of (*Qconv/Qrad*) as a function of T_r it is possible to collapse these three groups into a single curve. This was done by applying the results of the three groups in the square enclosure to the new dimensionless group, introduced in Eq. (28), above.

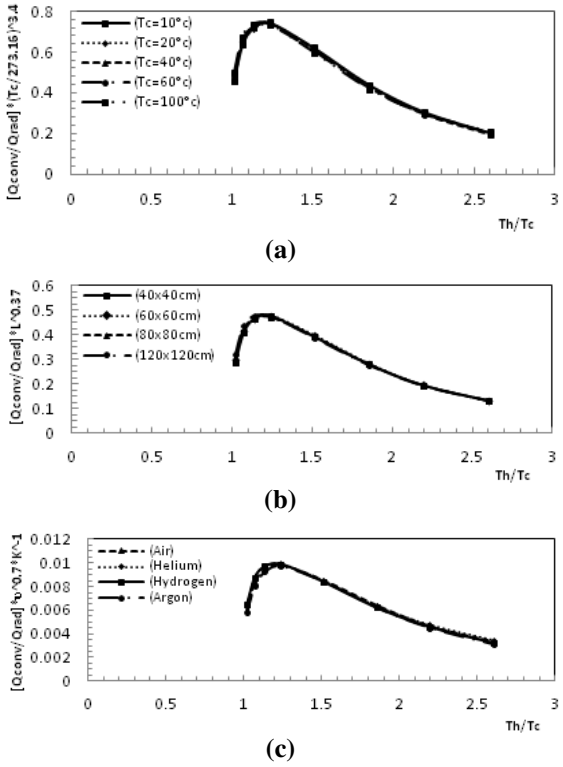

Fig. 6. Resultant Collapsed Curves for Different (a) Cold Wall Temperatures, (b) Enclosure Sizes and (c) Fluids.

The calculated results in the square enclosure of the new dimensionless group (*Qconv/Qrad*) using Eq. (28) for the three different groups were within an average deviation of 2.8% and a maximum deviation of 7.3%; compared to the numerical results. Using Eq. (28) to calculate (*Qconv/Qrad*) for the other two sets of parameters, (different sizes and different properties), gives an average deviation of less than 1.4% and a maximum deviation of less than 2.7%; compared to the numerical results. Fig. 7(b) shows the constants that were extracted to fit Eq. (28) to the data as a function of the temperature ratio T_r.

Also the calculated results in rectangular enclosure of the new dimensionless group (*Qconv/Qrad*) using Eq. (32) for the first regime with the three different groups were within an average deviation of 3.1% and a maximum deviation of 7.2%; compared to the numerical results. Also for the second regime with the three different groups the results were within an average deviation of 2.9% and a maximum deviation of 7.3%; compared to the numerical results. The comparison between numerical results of the new dimensionless group for each aspect ratio and the calculated empirical results using Eq. (32) for the two regimes caused by the changes in aspect ratio with using Eqs. (33) and are shown in Figs. 8(a) and 8(b). Finally Figs. 9(a) and 9(b) show the constants that were extracted to fit Eqs. (33) and (34) with Eq. (32) and to the data as a function of the temperature ratio T_r.

The turbulent natural convection without radiation interaction in the square enclosure has also been analysed and investigated numerically. The average Nusselt number at each temperature ratio for each case in the three different groups is recorded. Here, Eq. (27) was used to calculate the average Nusselt number for the turbulent natural convection without radiation interaction for the three different groups.

The calculated results of the average Nusselt number from Eq. (27) are found to be within an average deviation of 2.9% and a maximum deviation of 7.2% compared to the numerical predicted results. Fig. 7(a) shows the constants of Eq. (27) as a function of the temperature ratio T_r.

Also the calculated results in the rectangular enclosure of the average Nusselt number from Eq. (29) for the first regime are found to be within an average deviation of 2.7% and a maximum deviation of less than 7.3% compared to the numerical predicted results. Also for the second regime with the three different groups the results were within an average deviation of 3.2% and a maximum deviation of 6.6%; compared to the numerical results.

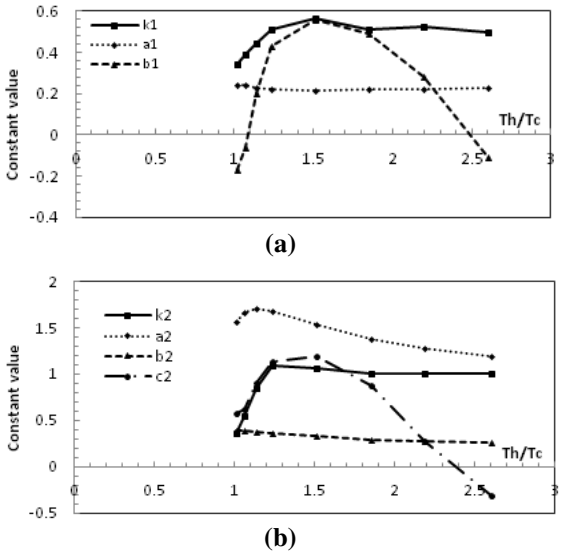

Fig. 7. Constants Values as a Function of T_h/T_c of (a) Natural Convection without Radiation Eq. (27), (b) Natural Convection with Interaction of Surface Thermal Radiation Eq. (28).

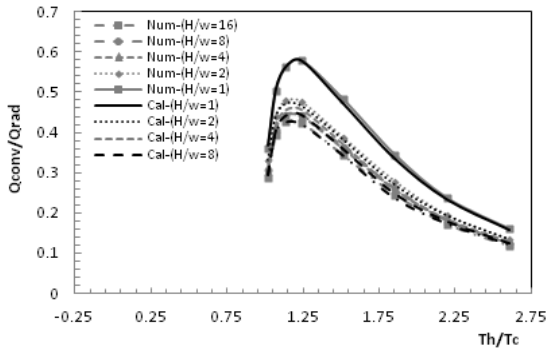

(a)

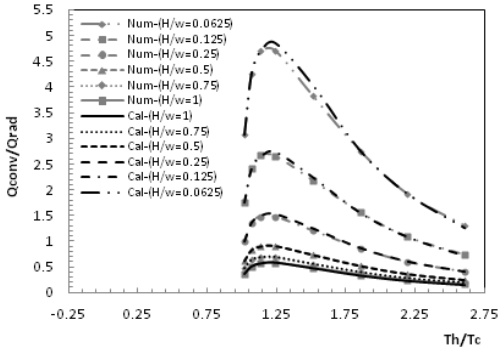

(b)

Fig. 8. Comparison between Numerical (num) and Empirical Calculated Results (cal) of Natural Convection with Radiation Interaction for: a) the First Regime and b) the Second Regime.

The comparison between the numerical results of the average Nusselt number for each aspect ratio and the calculated empirical results using Eq. (29) for the two regime of aspect ratio with using Eqs. (30) and (31) are shown in Figs. 10(a) and 10(b). From the figure the numerical and the calculated curves collapsed together. The Nusselt number, as a function of temperature ratio, is increases for all aspect ratios to a certain value of T_r then it starts to decrease. Figs. 11(a) and 11(b) shows the constants, as a function of temperature ratio T_r, that were extracted and used with Eqs. (30) and (31).

As a result, using Eq. (27) with the constants given in Fig. 7(a), to calculate the average Nusselt number in the square enclosure, with different sizes, temperatures and properties; for the range of $1.01 \leq \frac{T_h}{T_C} \leq 2.6$ and $1 \times 10^8 \leq R_a \leq 1 \times 10^{10}$ will give an average deviation of 2.9% and a maximum deviation of 7.2%; compared to the numerically predicted results.. Also using Eq. (28) with the constants given in Fig. 7(b), to calculate the ratio of convection to radiation heat transfer (the new dimensionless group) in the square enclosure with different sizes, temperatures and properties for the range of $1.01 \leq \frac{T_h}{T_C} \leq 2.6$ and $1 \times 10^8 \leq R_a \leq 1 \times 10^{10}$ will give an average deviation of 2.8% and a maximum deviation of 7.3%; compared to the numerical results.

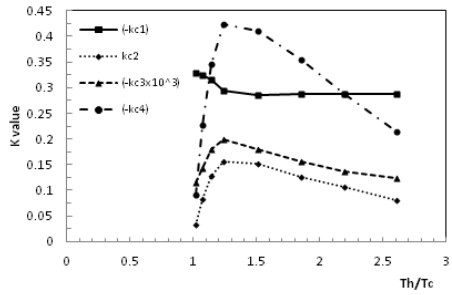

(a)

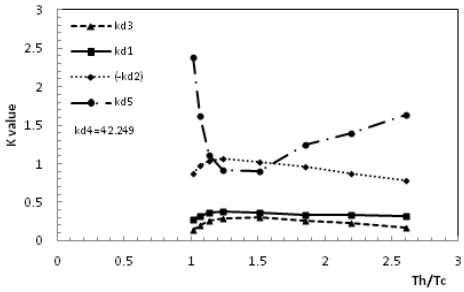

(b)

Fig. 9. Constants as a Function of Temperature Ratio of: a) Eq. (33) and b) Eq. (34).

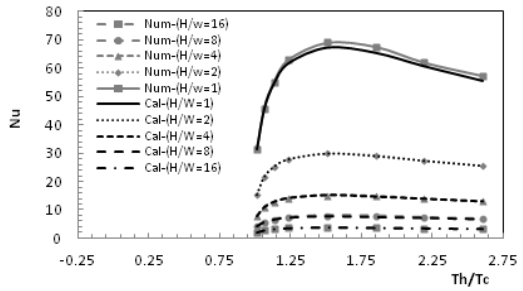

(a)

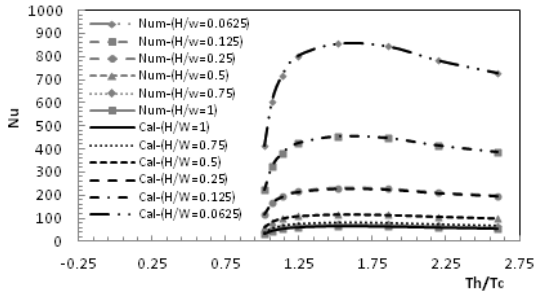

(b)

Fig. 10. Comparison between Numerical (num) and Empirical Calculated Average Nusselt Number (cal) of Pure Natural Convection for: a) First Regime and b) Second Regime.

Also using Eq. (29) with the constants given in Figs. 11(a) and 11(b) for the two regimes, to calculate the average Nusselt number in the rectangular enclosure, with different sizes, temperatures, aspect ratios and properties; for the range of $1.01 \leq \frac{T_h}{T_C} \leq 2.6$ and $2.5 \times 10^4 \leq \mathrm{R_a} \leq 5 \times 10^{12}$ will give an average deviation of less than 3.2% and a maximum deviation of less than 7.3% for the two regimes; compared to the numerically predicted results. Additionally, using Eq. (32) with the constants given in Figs. 9(a) and 9(b) for the two regimes, to calculate the ratio of convection to radiation heat transfer (the new dimensionless group) in the rectangular enclosure with different sizes, temperatures, aspect ratios and properties for the range of $1.01 \leq \frac{T_h}{T_C} \leq 2.6$ and $2.5 \times 10^4 \leq \mathrm{R_a} \leq 5 \times 10^{12}$ will give an average deviation of less than 2.9% and a maximum deviation of less than 7.3%; compared to the numerical results.

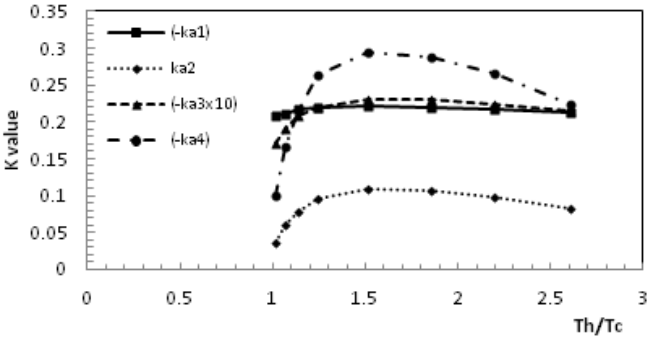

(a)

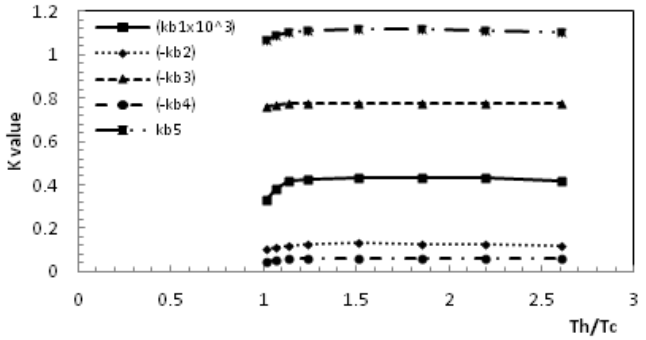

(b)

Fig. 11. Constants as a Function of Temperature Ratio of: a) Eq. (30) and b) Eq. (31).

5. Conclusions

The problem of turbulent natural convection with the interaction of surface thermal radiation in square and rectangular enclosures have been analysed with different fluids, enclosure sizes, aspect ratios and cold and hot wall temperatures. The problem was solved using variable fluid properties. Analysis starting from the PDE's that defined the system was carried out to find a relation between the natural convection and thermal radiation in the square enclosure.

The main conclusions from this study can be summarized as follows:

- The new dimensional group as a function of temperature ratio decreases slightly as the aspect ratio increases and it increases dramatically as the aspect ratio decreases.
- The ratio between the convection and radiation heat transfer is increased by increasing the temperature ratio up to a temperature ratio of 1.2; then this ratio starts to decrease. It was shown that the ratio between Rayleigh number and Nusselt number follows a similar trend.
- Correlation equations are provided to calculate the average Nusselt number as a function of Grashof and Prandtl numbers for the turbulent natural convection in square enclosure without radiation interaction. The calculated results using the correlation equations had a maximum error of 7.2% for the three different groups for the square enclosure, compared to the numerical results.
- The calculated results in rectangular enclosure of the average Nusselt number using the correlation equations for the first regime had an average deviation of 2.7% and a maximum deviation of less than 7.3% and for the second regime had an average deviation of 3.2% and a maximum deviation of 6.6%.
- The correlation equation for the new dimensionless group to predict the relation between convection and radiation in the square enclosure had a maximum error of 2.7% when it used for different fluid properties and enclosure sizes and a maximum error of 7.3% when the effect of cold wall temperature was included.
- The provided correlation equation for the new dimensionless group to predict the relation between convection and radiation heat transfer as a function of temperature ratio in the rectangular enclosure had an average deviation of 3.1% and a maximum deviation of 7.2% for the first regime and an average deviation of 2.9% and a maximum deviation of 7.3% for the second regime.
- The authors believe this to be a useful technique, as, by using the results it is possible to generalise the heat transfer in square and rectangular cavities filled with ideal gases.

References

1. Sharma, Anil Kumar; Velusamy, K.; and Balaji, C. (2008). Interaction of turbulent natural convection and surface thermal radiation in inclined square enclosures. *Heat Mass Transfer*, 44(10), 1153-1170.
2. Lankhorst, A.M. (1991). *Laminar and turbulent natural convection in cavities*. PhD Thesis. Delft University of Technology, the Netherlands.
3. Markatos, N.C.; and Pericleous K.A. (1984). Laminar and turbulent natural convection in an enclosed cavity. *International Journal of Heat and Mass Transfer*, 27(5), 755-772.
4. De Vahl Davis, G. (1983). Natural convection of air in a square cavity a bench mark numerical solution. *International Journal for Numerical Methods in Fluids*, 3, 249-264.

5. Barletta, A.; Nobile, E.; Pinto, F.; Rossi di Schio, E.; and Zanchini, E. (2006). Natural convection in a 2D-cavity with vertical isothermal walls: cross-validation of two numerical solutions. *International Journal of Thermal Sciences*, 45(9), 917-922.
6. Ramesh, N.; and Venkateshan, S.P. (2001). Experimental study of natural convection in a square enclosure using differential interferometer. *International Journal of Heat and Mass Transfer*, 44(6), 1107-1117.
7. Lankhorst, A.M.; Angirasa, D.; and Hoogendoorn, C.J. (1993). LDV Measurements of buoyancy-induced flows in an enclosure at high Rayleigh numbers. *Experimental Thermal and fluid Science*, 6(1), 74-79.
8. Nor Azwadi, C.S.; and Tanahashi, T. (2007). Three-dimensional thermal lattice Boltzmann simulation of natural convection in a cubic cavity. *International Journal of Modern Physics B*, 21(1), 87-96.
9. Henkes, R.A.W.M.; Van Der Vlugt, F.F., and Hoogendoorn, C.J. (1991). Natural-convection flow in a square cavity calculated with low-Reynolds number turbulence models. *International Journal of Heat and Mass Transfer*, 34(2), 377-388.
10. Henkes, R.A.W.M.; and Hoogendoorn, C.J. (1995). Comparison exercise for computations of turbulent natural convection in enclosures. *Numerical Heat Transfer, Part B*, 28(1), 59-78.
11. Balaji, C.; and Venkateshan, S.P. (1994). Correlations for free convection and surface radiation in a square cavity. *International Journal of Heat and Mass Transfer*, 15(3), 249-251.
12. Swarnendu Sen; and Sarkar, A. (1995). Effects of variable property and surface radiation on laminar natural convection in a square enclosure. *International Journal of Numerical Methods for Heat & Fluid Flow*, 5(7), 615-627.
13. Velusamy, K.; Sundararajan, T.; and Seetharamu, K.N. (2001). Interaction effects between surface radiation and turbulent natural convection in square and rectangular enclosures. *ASME Journal of Heat Transfer*, 123(6), 1062-1070.
14. Colomer, G.; Costa, M.; Consul, R.; and Oliva, A. (2004). Three-dimensional numerical simulation of convection and radiation in a differentially heated cavity using the discrete ordinates method. *International Journal of Heat and Mass Transfer*, 47(2), 257-269.
15. Kumar, P.; and Eswaran, V. (2010). A numerical simulation of combined radiation and natural convection in a differential heated cubic cavity. *Journal of Heat Transfer*, 132(2), 023501-13.
16. Elsherbiny, S.M.; Raithby, G.D.; and Hollands, K.G.T. (1982). Heat transfer by natural convection across vertical and inclined air layers. *ASME Journal of Heat Transfer*, 104, 96-102.
17. Shati , A.K.A.; Blakey, S.G.; and Beck , S.B.M. (2011). The effect of surface roughness and emissivity on radiator output. *Energy and Buildings*, 43(2-3), 400-406.
18. Patterson, J.; and Imberger, J. (1980). Unsteady natural convection in rectangular cavity. *Journal of Fluid Mechanics*, 100(1), 65-86.

19. Bejan, A. (1995). *Convection heat transfer*. 2nd (Ed.). New York: John Wiley & Sons Inc.
20. Zhang, T.; Ladeinde, F.; Zhang, H.; and Prasad, V. (1996). Comparison of turbulence models for natural convection in enclosures: applications to crystal growth processes. *ASME, Heat Transfer Division, Proceedings of 31st National Heat Transfer Conference*, 323, 17-26.
21. Zhang, Z.; Zhang, W.; Zhai, Z.; and Chen, Q. (2007). Evaluation of various turbulence models in predicting airflow and turbulence in enclosed environments by CFD: Part 2 - Comparison with experimental data from literature. *HVAC&R Research*, 13(6), 871-886.
22. FLUENT Inc. (2001). FLUENT 6 User's Guide, Lebanon, NH.
23. Johnstone, R.E.; and Thring, M.W. (1957). *Pilot plants, models, and scale-up methods in chemical engineering*. New York: McGraw-Hill.
24. Cheesewright, R.; King, K.J.; and Ziai, S. (1986). Experimental data for the validation of computer codes for the prediction of two-dimensional buoyant cavity flows. *Proc. ASME Meeting HTD*-60, 75-81.
25. King, K.J. (1989). *Turbulent natural convection in rectangular air cavities*. PhD Thesis, Queen Mary College, London, UK.